Theor Appl Genet (2000) 101:1180–1188

S. Kitamura · M. Inoue · N. Ohmido · K. Fukui

Quantitative chromosome maps and rDNA localization in the T subgenome of *Nicotiana tabacum* L. and its putative progenitors

Received: 25 October 1999 / Accepted: 24 March 2000

Abstract Using DAPI-stained prometaphase chromosomes, quantitative idiograms were constructed for the T subgenome of *Nicotiana tabacum* (2n = 4*x* = 48, SSTT) and two putative candidates for its T subgenome progenitor, *Nicotiana otophora* and *Nicotiana tomentosiformis* (both have 2n = 24, TT). The large chromosomes of the three karyotypes could be identified from the distributional pattern of the DAPI signal. Fluorescence in situ hybridization (FISH) with 5S rDNA gave not only good cytogenetical landmarks for identification of small chromosomes of the karyotypes but also phylogenetical information. In all three idiograms, 5S rDNA was localized in the proximal region of the long arm of a small submetacentric pair, but an additional 5S rDNA locus was detected terminally on the short arm of a small metacentric pair in *N. otophora*. The 18S rDNA locus detected here corresponded to satellite regions in all three karyotypes. Two satellited pairs in *N. otophora* and one satellited pair in *N. tomentosiformis* had single large subterminal DAPI blocks and two interstitial DAPI bands on their long arms, respectively. For the T subgenome component of *N. tabacum*, the single intense DAPI band was depicted on the center of the long arm of a satellited pair in the idiogram, although two interstitial bands were often detected on the long arm of the satellited pair in some spreads. Therefore, it was suggested that the T component of *N. tabacum* was more similar to that of *N. tomentosiformis* than *N. otophora*, especially in respect of the number and location of rDNA and the distributional patterns of DAPI signals.

Keywords Quantitative idiogram · Prometaphase chromosome · Image analysis · Fluorescence in situ hybridization · T subgenome progenitor

Communicated by Y. Gleba

S. Kitamura · M. Inoue (✉)
Laboratory of Plant Breeding Science, Faculty of Agriculture, Kyoto Prefectural University, Sakyo, Kyoto 606–8522, Japan
Tel. & Fax: +81-75-703 5603

N. Ohmido
Laboratory of Genetic Engineering, Hokuriku National Agricultural Experiment Station, Inada, Joetsu 943–0193, Japan

K. Fukui
Department of Biotechnology, Faculty of Engineering, Graduate School of Osaka University, Yamada-Oka 2–1, Suita 565–0871, Japan

Introduction

Nicotiana tabacum L., cultivated tobacco, has long been utilized as a model plant in breeding and genetic investigations, because the management of its cultivation is easy and a procedure for its in vitro development has been established. Such advantages also give great worth to this species as a transgenic model plant. On the other hand, the amphidiploidy of the *N. tabacum* genome (SSTT) has led many investigators to study the origin of the respective subgenomes. Both genetic and molecular research support the concept that the S subgenome donor is most closely related to the present-day *Nicotiana sylvestris* of the extant wild species (Gerstel 1960, 1963; Okamuro and Goldberg 1985). Analysis of the mitochondrial genome (Bland et al. 1985) and Fraction-I protein (Gray et al. 1974) implies that a species close to *N. sylvestris* is the maternal parent. The T subgenome donor species has been restricted to closely related to extant core species of the Tomentosae section. It is considered that the most likely candidate for the T subgenome progenitor of *N. tabacum* is either *Nicotiana otophora* (Goodspeed 1954), *Nicotiana tomentosiformis* (Sheen 1972), or introgressive hybrids among the Tomentosae section (Kenton et al. 1993).

Chromosome analysis in *N. tabacum* is laborious and time-consuming due to the large number of chromosomes and their morphological similarity. Goodspeed (1954) described karyotypic features of *N. tabacum* and other *Nicotiana* species in detail as revealed by conventional cytological methods. Recent advances in molecular cytogenetics have made it possible to detect land-

marks on *N. tabacum* chromosomes (Parokonny and Kenton 1995). Moscone et al. (1996) reported that at least 20 pairs could be discriminated from 24 pairs of *N. tabacum* chromosomes by in situ hybridization and DAPI banding methods. However, because karyotypes at the somatic metaphase stage were quite similar between Tomentosae species, especially *N. otophora* and *N. tomentosiformis*, comparative chromosome analysis for the T subgenome progenitors was not sufficient.

It is known that the use of prometaphase cells is effective for the identification of individual chromosomes because characteristics caused by the uneven condensation of chromatin fibers along chromosomes are more prominent at this stage (Fukui and Mukai 1988). The chromosome image analyzing system, CHIAS, which has been developed up to the third-generation (Fukui 1986; Nakayama and Fukui 1997; Kato and Fukui 1998), is suitable for the measurement of the condensation pattern (CP) of prometaphase chromosomes. In fact, using the CP of prometaphase chromosomes obtained with CHIAS, reliable quantitative chromosome maps were developed in rice (Fukui and Iijima 1991), *Brassica* (Fukui et al. 1998), sugarcane (Ha et al. 1999) and spinach (Ito et al. 2000), in all of which complete chromosome identification was difficult at mid-metaphase. Kamisugi et al. (1993) statistically demonstrated that the CP measured with CHIAS at prometaphase was a representative image parameter of chromosome morphology.

In this paper, CHIAS III was applied to the measurement of DAPI intensities along each chromosome at the somatic prometaphase stage in order to construct quantitative idiograms of the T subgenome component of *N. tabacum* and two putative candidates for the T subgenome progenitor, *N. otophora* and *N. tomentosiformis*. In addition, 18S and 5S ribosomal RNA genes (rDNA) were physically localized on the developed idiograms by fluorescence in situ hybridization (FISH).

Materials and methods

Plant materials and chromosome preparation

N. otophora Grisebach (2n = 2*x* =24, TT), *N. tomentosiformis* Goodspeed (2n = 2*x* = 24, TT) and *N. tabacum* L. cv Bright Yellow 4 (BY-4; 2n = 4*x* = 48, SSTT) were used for cytogenetical investigations. They were cultivated in a greenhouse maintained at about 25°C with a natural day length. *N. sylvestris* Spegazzini & Comes (2n = 2*x* = 24, SS), in the Alatae section, was also grown for the purpose of extracting total genomic DNA for genomic in situ hybridization (GISH) analysis.

Root tips were harvested from vigorous plants potted in sterilized soil. Then they were brushed softly, immersed in 2 mM of 8-hydroxyquinoline, decompressed for 5 min, and incubated at 18°C for 2 h. After fixation in 3 : 1 of ethanol : acetic acid solution at 4°C for up to 2 days, they were stored in 70% ethanol at 4°C. Using those samples, chromosome preparation was carried out by the enzymatic maceration/air drying (EMA) method (Fukui and Iijima 1992; Fukui 1996). Until utilization for in situ hybridization analysis, glass slides with well-spread chromosomes were kept desiccated at –20°C.

Probe preparation

Total genomic DNA was isolated from about 10 g of fresh leaves of *N. otophora*, *N. tomentosiformis*, *N. tabacum* and *N. sylvestris* using the CTAB procedure (Murray and Thompson 1980). For use as probes, they were labeled with either biotin-16-dUTP or digoxigenin-11-dUTP by the random primed labeling method according to the manufacturer's instructions (Boehringer Mannheim).

Amplification of 18S and 5S rDNA sequences was carried out with total genomic DNA from *N. tabacum*, using a pair of primers 5'-AAC GGC TAC CAC ATC CAA GG-3' and 5'-GGT GGT GCC CTT CCG TCA AT-3' for 18S rDNA, and 5'-CGA TCA TAC CAG CAC TAA CG-3' and 5'-TAC TAC TCT CGC CCA AGC AC-3' for 5S rDNA. PCR was performed in volumes of 100 µl containing 1 × PCR buffer (Perkin Elmer; contains 1.5 mM $MgCl_2$), 1 µM each of a pair of primers, 200 µM each of dATP, dGTP, dCTP and dTTP, 10–100 ng of template DNA, and 2.5 U of *Taq* DNA polymerase (Ampli*Taq* Gold, Perkin Elmer). After a first denaturation step of 10 min at 94°C, 40 amplification cycles at 94°C for 1 min, 57°C (for 18S rDNA) or 50°C (for 5S rDNA) for 1 min and 72°C for 3 min, were performed followed by a final extension step of 10 min at 72°C. Labeled rDNA probes were obtained by the PCR direct labeling method (Fukui et al. 1994), with 70% or 30% substitution of biotin-16-dUTP or digoxigenin-11-dUTP for dTTP, respectively.

In situ hybridization

The procedure of in situ hybridization was conducted according to Shishido et al. (1998) with some modifications. Chromosome spreads were treated with 100 ng/µl of RNase at 37°C for 1 h. The hybridization mixture consisted of 50% formamide, 2 × SSC and labeled DNA probes at a final concentration of 11.4 ng/µl for genomic DNA and 5.8 ng/µl for rDNA. For FISH with rDNA, salmon sperm DNA was added as a blocking reagent to the hybridization mixture adjusted to a 100-fold concentration against probes. The mixture was denatured at 90°C for 10 min and cooled down on ice immediately. A 15-µl aliquot of the hybridization mixture was applied onto each slide, covered with a coverslip, and sealed with rubber cement. Both chromosomal DNA and probe DNA on the slides were denatured together on the heat block at 80°C for 5 min, and hybridized with each other at 37°C for 1–2 nights in a humid dark box. Signal amplification and detection of hybridization sites were performed with biotinylated anti-avidin-D and avidin-FITC for the biotinylated probe, and with rhodamine-labeled anti-digoxigenin raised in sheep and Texas red-labeled anti-sheep IgG for the digoxigenin-labeled probe, respectively. After a final detection step, washing was carried out twice in BT buffer (0.1 M sodium hydrogen carbonate, 0.05% Tween-20) and once in 2 × SSC at 37°C for 10 min each. Chromosomal DNA was counterstained with DAPI in an antifadant solution (Kitamura et al. 1997). Fluorescent signals were observed with a fluorescence microscope equipped with UV-, B-, and G-excitation filters, captured digitally and separately, with a different excitation light, using a cooled CCD camera (PXL1400, Photometrics). The captured images derived from the same spread were integrated on a personal computer using graphic software, IP-Lab (Photometrics) and Photoshop (Adobe). When necessary, sequential FISH was performed according to Hanson et al. (1996).

Image analysis

Among the captured DAPI images, prometaphase chromosome spreads with a similar degree of condensation and with non-superimposition of individual chromosomes were subjected to image analysis (CHIAS III; Kato and Fukui 1998). The main frame of this analyzing system is a public domain software, NIH Image (developed at the U.S. National Institutes of Health and available via the Internet at http://rsb.info.nih.gov/nih-image/). Image analysis was performed according to the detailed stepwise procedures

of Kato et al. (1997). Individual chromosomes were identified by visual inspection, then DAPI intensities along chromosomes were converted to numerical data, for the development of quantitative idiograms.

Results

Features of prometaphase chromosomes stained with DAPI

By means of Giemsa staining of metaphase spreads, it was confirmed that both genotypes of *N. otophora* and *N. tomentosiformis* currently used had two sets of a chromosome complement consisting of five large subtelocentric and seven small meta- to submeta-centric chromosomes (data not shown). These bimodal constitutions were consistent with previous reports (Goodspeed 1954; Ogura 1980; Parokonny and Kenton 1995). Of the five large subtelocentric pairs, two exhibited secondary constrictions in *N. otophora* and one in *N. tomentosiformis*. No satellited chromosome was observed within the seven small chromosomes of these two species.

The prometaphase chromosome spreads stained with DAPI are shown in Fig. 1. In both *N. otophora* (Fig. 1A) and *N. tomentosiformis* (Fig. 1B), blocks with an intense DAPI signal were detectable on five large subtelocentric pairs, some of which were rarely visualized at metaphase. Among those subtelocentric pairs, there were some differences in the patterns of DAPI signals. In *N. otophora*, two large subtelocentric pairs possessed extensive DAPI blocks at the end to center of the long arms. In contrast, the blocks with an intense DAPI signal were relatively small in the other three subtelocentric pairs, and observed in subterminal regions of their long arms. In *N. tomentosiformis*, two out of five large subtelocentric pairs emitted bright blue fluorescence at the end to the center of their long arms. As shown in *N. otophora*, the remaining three subtelocentric pairs of *N. tomentosiformis* had subterminal and/or interstitial DAPI blocks on their long arms. With respect to two pairs with terminal DAPI blocks, the patterns of strong DAPI signals in *N. otophora* were similar to those in *N. tomentosiformis*. For the other three subtelocentric pairs, in contrast, interspecific differences were obvious in DAPI patterns. For instance, two DAPI bands were observed at interstitial regions of a subtelocentric pair in *N. tomentosiformis* (Fig. 1B, arrow), which was never detected in *N. otophora*.

At metaphase, seven small meta- to submeta-centric pairs did not show specific DAPI bands available for the discrimination of each chromosome pair in *N. otophora* and *N. tomentosiformis*. The employment of prometaphase spreads made it possible to detect differences in length, arm ratio, and DAPI banding pattern among small components in the two species. One medium-sized pair in the overall chromosome set was readily identified by centromeric and terminal DAPI bands on the long arm in both species. One pair in *N. tomentosiformis* constantly exhibited a specific DAPI pattern, a conspicuous DAPI block on the long arm. Regardless of the lack of a molecular cytogenetical marker, the smallest pair among the remaining chromosomes was also identified by size in both *N. otophora* and *N. tomentosiformis*. However, it was difficult to discriminate other small pairs by only visual inspection due to their morphological similarity and the absence of distinctive fluorescent signals.

To discriminate between the two subgenome components (S and T), multicolor GISH (McGISH) was carried out on *N. tabacum* cv Bright Yellow 4 chromosomes using biotinylated *N. tomentosiformis* DNA and digoxi-

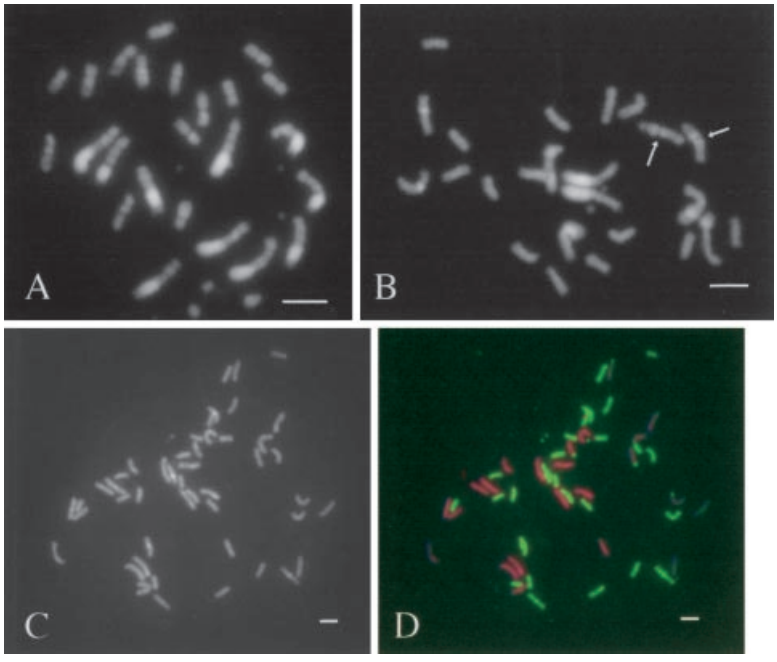

Fig. 1A–D Prometaphase chromosome spreads of T genome relatives in *Nicotiana*. **A**, **B** and **C** DAPI images of *N. otophora* (**A**), *N. tomentosiformis* (**B**) and *N. tabacum* cv Bright Yellow 4 (BY-4, **C**). **D** McGISH of **C**. Hybridization signals of total genomic DNA from *N. sylvestris* and *N. tomentosiformis* are visualized as *red* and *yellow-green*, respecitvely. *Arrows* in **B** indicate unique chromosomes with two DAPI bands on their long arms. Scale bars represent 5 μm

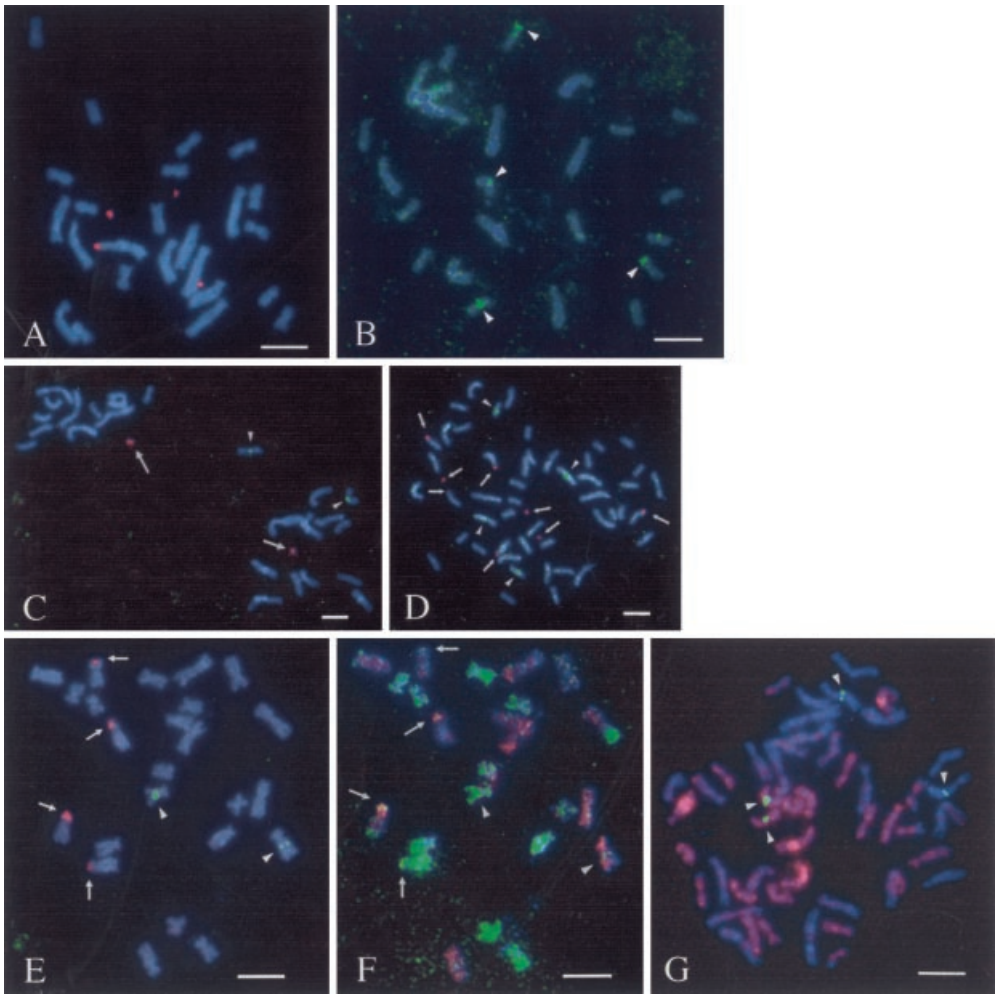

Fig. 2A–G FISH of T genome relatives. **A** and **B** Hybridization with 18S rDNA (**A**) and 5S rDNA (**B**) to prometaphase chromosomes of *N. otophora*. **C** and **D** Multicolor FISH (McFISH) with 18S (*red*) and 5S (*yellow-green*) rDNA to prometaphase chromosomes of *N. tomentosiformis* (**C**) and *N. tabacum* cv BY-4 (**D**). **E** McFISH with 18S (*red*) and 5S (*yellow-green*) rDNA to metaphase chromosomes of a haploid plant derived from anther culture of BY-4. **F** Sequential McGISH of **E** with total genomic DNA from *N. sylvestris* (*red*) and *N. tomentosiformis* (*yellow-green*). **G** Simultaneous FISH with *N. tomentosiformis* genomic DNA (*red*) and 5S rDNA (*yellow-green*) to prometaphase chromosomes of BY-4. Each scale bar represents 5 μm

genin-labeled *N. sylvestris* DNA as probes (Fig. 1C, D). As shown in Fig. 1D, hybridization with *N. tomentosiformis* DNA was visualized as a yellow-green signal, and that with *N. sylvestris* DNA as red. For the purpose of comparison with the T genome species mentioned above, we focused on the T subgenome component with yellow-green signals in this study. In all spreads observed, there were 20 chromosomes with yellow-green signals along their entire length and eight chromosomes with signals in segments. For these eight bicolored chromosomes, where translocations had occurred between subgenomes, homologous pairs were determined based on the hybridization patterns of each genomic DNA, and assigned to either the S or T subgenome according to the color of signals by which more than half the length of each chromosome was labeled. As a consequence, two bicolored pairs were defined as chromosomes originated from the T subgenome in this study. Among T subgenome chromosomes, two larger subtelocentric pairs showed intense DAPI fluorescence in their long arms (Fig. 1C, D). The uneven distribution of hybridization signals with *N. tomentosiformis* DNA along chromosomes (Kenton et al. 1993) sometimes allowed for the identification of several chromosomes. As in T genome species, however, the determination of homologues was difficult in some meta- to submeta-centric pairs.

Localization of 18S and 5S rDNA in prometaphase chromosomes

Chromosomal localization of 18S and 5S rDNA was determined by FISH. The 18S rDNA probe (approximately 750 bp) was amplified from *N. tabacum* DNA. The pair of primers used here was designed from the coding sequence of rice 17S rDNA, and the annealing position of each primer showed approximately 100% homology among the rDNA sequences of rice, yeast, rat and *Xenopus laevis* (Takaiwa et al. 1984). Four strong hybridization signals of the 18S rDNA probe were detected in *N. otophora* (Fig. 2A). It was revealed that these strong signals corresponded to four satellite regions by integration with the DAPI-counterstained image. In *N. tomentosiformis*, two strong signals were observed, and their sites were also located in two satellites (Fig. 2C).

As shown in Fig. 2D and E, hybridization of the 18S rDNA probe occurred on four pairs (arrows) in *N. tabacum*. A difference in signal intensity was often observed

among these four loci, reflecting a difference in the copy number of repeat units in each locus. In the chromosome set of haploid plants of *N. tabacum*, four signals were observed (Fig. 2E, arrows). Furthermore, sequential McGISH demonstrated that the S subgenome had three signals (Fig. 2F). Therefore, of these four loci in *N. tabacum*, one was demonstrated to occur in T subgenome chromosomes by GISH analysis (Fig. 2E, F). This locus also coincided with the satellite of the T subgenome component.

FISH signals of the 5S rDNA probe were examined in T genome relatives. The 5S rDNA probe was also amplified from *N. tabacum* DNA, using a pair of primers designed from the consensus sequence of tobacco 5S rDNA (Fulneček et al. 1998). Southern hybridization was preliminarily performed using this probe (72-bp in length), and it was ascertained that *N. otophora*, *N. tomentosiformis* and *N. tabacum* shared approximately the same band of 600—650 bp (data not shown). Four and two signals were constantly observed in *N. otophora* (Fig. 2B, arrowheads) and *N. tomentosiformis* (Fig. 2C, arrowheads), respectively. Superimposition with the DAPI image revealed the precise chromosomal localization of the 5S rDNA sites at the somatic prometaphase stage. In *N. otophora*, the 5S rDNA was localized on two pairs of small chromosomes (Fig. 2B). Among two 5S rDNA loci in *N. otophora*, one occurred in the proximal region of the long arm of a submetacentric pair, and the other in the terminal region of the short arm of a metacentric pair. On the other hand, in *N. tomentosiformis*, FISH signals with 5S rDNA were detected in the proximal region of the long arm of a small submetacentric pair (Fig. 2C). The 5S rDNA locus in *N. tomentosiformis* appeared to be identical to one of the two loci in *N. otophora*.

Two pairs with 5S rDNA were found in prometaphase chromosomes of *N. tabacum* (Fig. 2D, arrowheads). Sequential GISH following 5S rDNA FISH (Fig. 2E, F), and simultaneous FISH with 5S rDNA and *N. tomentosiformis* genomic DNA (Fig. 2G), revealed that each subgenome of *N. tabacum* possessed one 5S rDNA locus. The location in the S subgenome was the interstitial region of the long arm of a large subtelocentric pair, and that in the T subgenome was the proximal region of a small submetacentric pair (Fig. 2F, G). The 5S rDNA locus detected in T subgenome chromosomes seemed to be identical to that in *N. tomentosiformis* and one of the two loci in *N. otophora*.

Construction of quantitative idiograms

The quantitative idiograms were constructed using five prometaphase chromosome spreads stained with DAPI (Fig. 3). Conspicuous DAPI blocks recognized by fluorescence microscopy were precisely positioned on their idiograms.

In *N. otophora* and *N. tomentosiformis* idiograms (Fig. 3A, B), two pairs (chromosomes 1 and 2) exhibited more-distal, extensive DAPI blocks on their long arms. It was demonstrated that the DAPI pattern of the other three subtelocentric pairs (chromosomes 3, 4 and 5) was comparable in *N. otophora* but more unique in *N. tomentosiformis*. Chromosome 6 of both idiograms corresponded to the medium-sized pair. Chromosomes 7 and 9 in *N. otophora* and chromosome 9 in *N. tomentosiformis* were easily identified by the presence and position of 5S rDNA. One small metacentric pair (chromosome 12) in *N. tomentosiformis* corresponded to that with DAPI block on the long arm. Of the remaining pairs, the smallest pair identified by visual inspection was chromosome 12 and chromosome 11 in *N. otophora* and *N. tomentosiformis*, respectively. Although chromosomes 8, 10, and 11 in *N. otophora* and chromosomes 7, 8, and 10 in *N. tomentosiformis* showed few remarkable

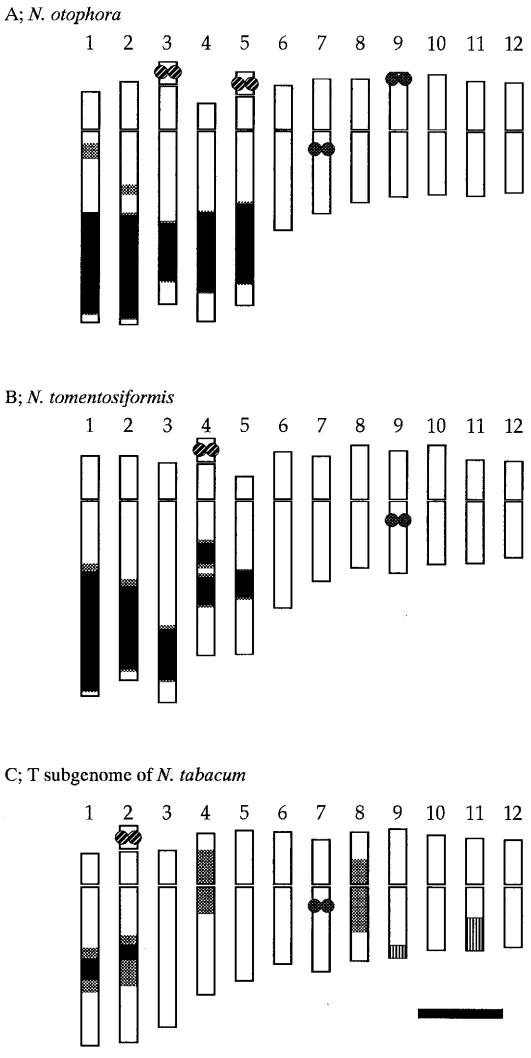

Fig. 3A–C Quantitative idiograms of three T (sub)genome karyotypes. **A** *N. otophora*, **B** *N. tomentosiformis*, **C** T subgenome component of *N. tabacum* cv BY-4. *Black*, *gray*, and *white areas* represent the most intense, intense, and weak fluorescence with DAPI, respectively. ▨ and ● indicate the location of 18S and 5S rDNA, respectively. *Vertical hatching regions* indicate S subgenome chromatin. Scale bar represents 5 μm

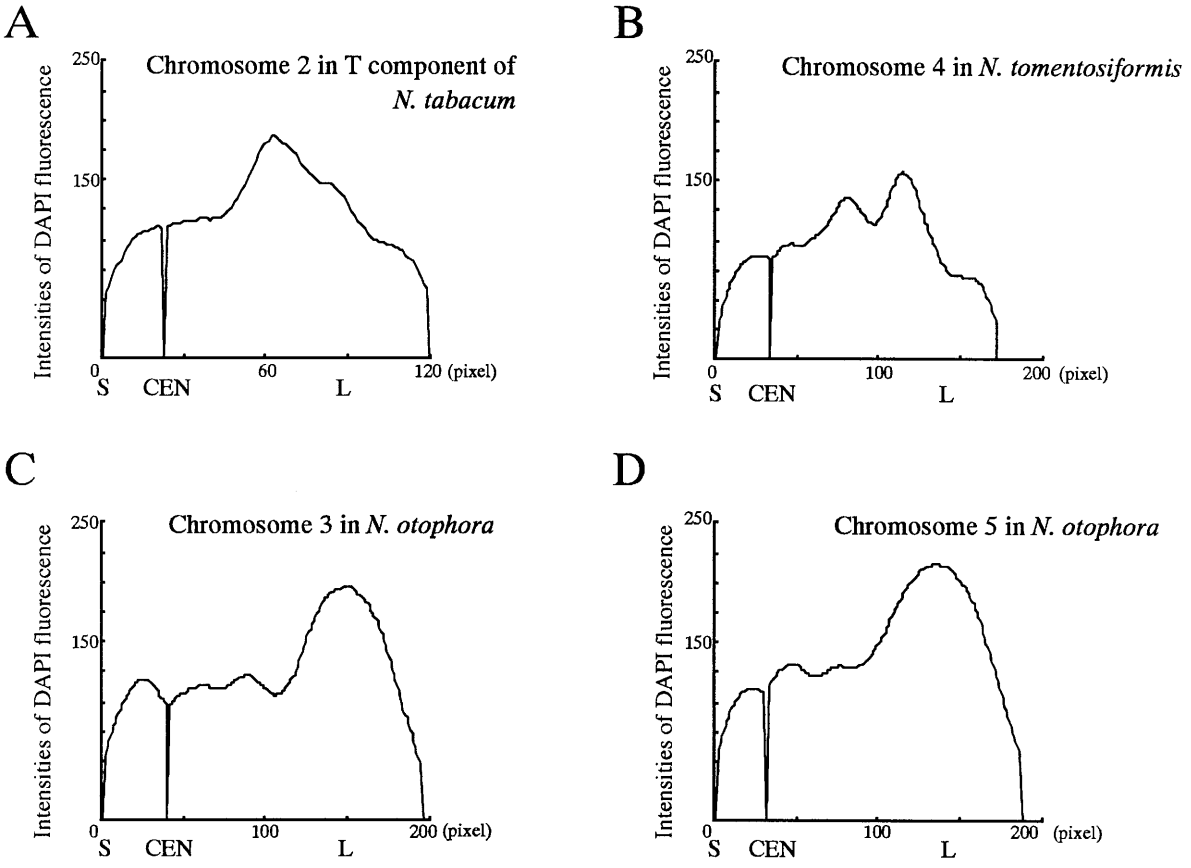

Fig. 4A–D DAPI profiles along the satellited chromosome pairs in T genome relatives. **A** T subgenome component of *N. tabacum* cv BY-4. **B** *N. tomentosiformis*. **C** Chromosome 3 in *N. otophora*. **D** Chromosome 5 in *N. otophora*. *S, L, and CEN* indicate short arm, long arm, and centromere, respectively. It should be noted that **A** was drawn in 11 pixels/μm, the others in 15 pixels/μm

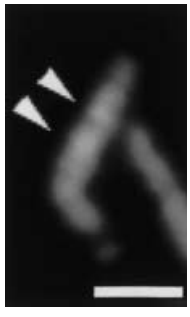

Fig. 5 Satellited chromosome of the T subgenome component of *N. tabacum* cv BY-4 with two DAPI bands (*arrowheads*) at interstitial regions of the long arm. Scale bar represents 3 μm

fluorescent signals, each chromosome was discriminated by chromosomal length and arm ratio.

For the T subgenome component of *N. tabacum* cv BY-4, it was confirmed that intense DAPI bands existed in intercalary regions of two T subgenome chromosome pairs (chromosomes 1 and 2). A difference in the width of the band between these two pairs was detected, shown as black areas in Fig. 3C. Chromosome 7 had a 5S rDNA locus on the long arm. Chromosomes 9 and 11 could be identified by the size of translocated chromatin from the S subgenome. Among the remaining chromosomes, one subtelocentric pair (chromosome 3) and two subtelo- to submeta-centric pairs (chromosomes 4 and 5) were identified by their relatively large size and arm ratio. The smallest pair was chromosome 12. However, identification was extremely difficult for chromosomes 6, 8, and 10, because clear marker signals and morphological differences were not detected among them. Further study on the gray region on chromosome 8 obtained from DAPI analysis is necessary.

The 18S and 5S rDNA loci were mapped in the idiograms. Chromosome pairs with 18S rDNA corresponded to satellited chromosomes in all three idiograms. While in *N. otophora* two pairs of satellited chromosomes had extensive subterminal DAPI blocks (Fig. 3A), in *N. tomentosiformis* a satellited pair had two DAPI bands on their long arm (Fig. 3B). In the idiogram of the T subgenome chromosomes of *N. tabacum* cv BY-4 (Fig. 3C), a satellited pair had a single, strong DAPI band on the center of its long arm. Figure 4 shows profiles of averaged DAPI intensities along the satellited chromosomes. Differences in DAPI intensity at the most prominent position and entire chromosomal length were observed among each of the satellited pairs, but the distributional DAPI pattern and the relative position of the prominent DAPI band in *N. tabacum* were similar to those in *N. tomentosiformis*. Considering the fact that two DAPI bands were sometimes observed in the interstitial region of the long arm of a satellited pair in the T component of *N. tabacum* (Fig. 5), the single black band on the satellited pair in the T component idiogram might be due to

the weaker fluorescence of the distal than the proximal band (Figs. 4, 5). On the other hand, in the small submetacentric pair with 5S rDNA in the proximal region, which was regularly observed in three karyotypes, a faint DAPI band presumably corresponding to the 5S rDNA locus was often detected. There was no DAPI-positive band at the terminal 5S rDNA site in *N. otophora*.

Discussion

In the present study, we made quantitative chromosome maps, at the prometaphase stage, of the T subgenome component of *N. tabacum* and its putative T subgenome progenitors, *N. otophora* and *N. tomentosiformis*. Studies on the chromosome features in *Nicotiana*, including these three species, have been carried out (Goodspeed 1954; Merritt 1974; Kenton et al. 1993; Parokonny and Kenton 1995), in most of which metaphase chromosomes were investigated. In contrast, the use of prometaphase spreads in this study, made the features of each chromosome more visible. Furthermore, there was no significant difference in total chromosome length of each cell among the five spreads subjected to image analysis ($\alpha = 0.05$). For the representation of karyotypes, CHIAS III was used here (Kato and Fukui 1998).

It is well-known that karyotypic bimodality (large subtelocentrics and small meta- to submeta-centrics) is characteristic of the core species of the Tomentosae section (Goodspeed 1954; Ogura 1980). By the distributional patterns of conspicuous DAPI signals along chromosomes, the large subtelocentrics observed here are subdivided into two classes; one of them is composed of subtelocentrics with terminal DAPI blocks (class-1), the other with subterminal or interstitial blocks (class-2). Chromosomes 1 and 2 of *N. otophora* were mostly identical in DAPI pattern to those of *N. tomentosiformis*, respectively. In *N. kawakamii* Y. Ohashi, which has been placed in the core species of Tomentosae taxonomically (Ogura 1980; Reed 1991), two subtelocentric pairs with large terminal DAPI blocks were found (Nakamura et al., in preparation). On the other hand, class-2 subtelocentrics were more variable in terms of the position of conspicuous DAPI blocks among the core species. Therefore, it was suggested that two pairs of class-1 chromosomes had more limited characteristics for karyotypes of core species of Tomentosae, and also that karyotypic differences among members of the core species were largely attributed to the differences of variable class-2 subtelocentrics.

In T subgenome chromosomes of *N. tabacum* cv BY-4, there were class-2 but not class-1 subtelocentrics (Fig. 3C). The class-1 subtelocentrics were not detected in the T component of other two cultivars of *N. tabacum* (Moscone et al. 1996). Therefore, it is inferred that two class-1 pairs have been rearranged during the development of the present tobacco genome, or else that the terminal DAPI blocks of those pairs had been reduced in the progenitor of the T subgenome prior to hybridization of the S and T subgenomes. Alternatively, sequences in DAPI-positive regions may be increased specifically in core species of Tomentosae after divergence within the Tabacum subgenus. In this study, most of the DAPI-positive blocks were also stained with chromomycin A_3 (data not shown), indicating that they corresponded to heterochromatin blocks, probably comprising several kinds of repetitive DNA sequences. Parokonny and Kenton (1995) used repetitive DNA as a probe for FISH, and suggested a translocation between the S and T subgenomes involving large subtelocentrics in the T subgenome. Analysis using other repetitive, especially species-specific, sequences would offer clues for the derivation of the large subtelocentrics in the *N. tabacum* T component.

Throughout our observations, hybridization signals of the 18S rDNA probe corresponded to satellite regions in *N. otophora* and *N. tomentosiformis*. The result for *N. tomentosiformis* was consistent with that of Kenton et al. (1993) using pTa71 probe. But for *N. otophora*, Kenton et al. (1993) have detected two pairs, each with a double rDNA site in the short arm, while our results showed two pairs each with a single rDNA site. This incongruity in the number of rDNA sites in *N. otophora* may be attributable to a difference in the degree of extension of DNA at the secondary constrictions.

In *N. tabacum* cv Bright Yellow 4, 18S rDNA sites were detected on four pairs of chromosomes, one of which was assigned to the T subgenome. Parokonny and Kenton (1995) described that, in *N. tabacum* cv SR-1 and 095–55, hybridization of pTa71 was observed on four pairs, and in cv 35466 and Samsun NN, on five pairs. Because the 18S rDNA loci in BY-4 appeared to be identical not only to those in SR-1, 095–55 (Parokonny and Kenton 1995) and cv Gatersleben (Moscone et al. 1996) but also to four out of five loci in 35466 and Samsun NN (Parokonny and Kenton 1995), one rDNA locus in the T component is likely to be conserved over cultivars. A pair with this rDNA site corresponded to a satellited chromosome pair, chromosome 2 in Fig. 3C. Parokonny and Kenton (1995) reported that in metaphase cells of *N. otophora*, a single DAPI band was detected at the center of long arm of the satellited chromosome, and also that a satellited pair of the T component of *N. tabacum* was similar to that of *N. otophora*. In the prometaphase cells of *N. otophora* used here, however, the prominent DAPI bands on two satellited chromosome pairs were subterminal (Fig. 3A). In addition to the idiograms (Fig. 3), the difference in DAPI-profiles of the satellited pair in *N. otophora*, *N. tomentosiformis* and *N. tabacum* (Fig. 4) suggests that one satellited pair (chromosome 2) of the T subgenome component of *N. tabacum* is more similar to that of *N. tomentosiformis* than that of *N. otophora*.

There were few landmarks on the small meta- to submeta-centric chromosomes of T genome relatives. The present FISH analysis with 5S rDNA provided a remarkable cyto-molecular landmark for the identification of small chromosomes. The 5S rDNA loci are also interest-

ing phylogenetically. In the present study, the number and location of 5S rDNA sites in the T subgenome component of *N. tabacum* were similar to those in *N. tomentosiformis*. In the allodiploid species *Allium wakegi* Araki, 5S rDNA loci appeared to correspond to those of two putative progenitors (Hizume 1994). Our preliminary FISH experiment with 5S rDNA on *N. sylvestris* chromosomes revealed a single locus on the long arm of a subtelocentric pair (data not shown), which corresponded to that of the S subgenome component of *N. tabacum* (Fig. 2E, G). Hence, it is suggested that chromosome rearrangement involving a segment with the major 5S rDNA locus has not taken place between the S and T subgenomes of *N. tabacum*. This suggestion is supported by the present results in which a hybridization signal with 5S rDNA has not been detected on eight translocated chromosomes of *N. tabacum* in spite of a long hybridization reaction. Hence, it seems that present-day *N. tomentosiformis* is more close to the T subgenome progenitor of *N. tabacum* than present-day *N. otophora* in terms of the 5S rDNA locus. As for 5S rDNA locus, Nakamura et al. (in preparation) found that *Nicotiana kawakamii* possessed two 5S rDNA loci similar to those in *N. otophora*. Here, we observed that one of two 5S rDNA loci in *N. otophora* was similar to that in the T subgenome of *N. tabacum* and *N. tomentosiformis*. Therefore, it is suggested that amplification and/or de-amplification of 5S rDNA clusters has taken place during the speciation of core species of the Tomentosae section prior to the formation of *N. tabacum*, as reported in cultivated amphidiploid cotton (*Gossypium hirsutum* L.) and its putative progenitor species (Hanson et al. 1996).

In conclusion, the idiograms based on the distributional patterns of DAPI-positive regions and rDNA sites indicate that the T subgenome of *N. tabacum* derived its origin from *N. tomentosiformis* rather than *N. otophora*. Further FISH with other new probes, and their sequence analysis, will facilitate elucidation of the evolutionary processes of each subgenome involved in alloploid formation.

References

Bland MM, Matzinger DF, Leving III CS (1985) Comparison of the mitochondrial genome of *Nicotiana tabacum* with its progenitor species. Theor Appl Genet 69: 535–541

Fukui K (1986) Standardization of karyotyping plant chromosomes by a newly developed chromosome image analyzing system (CHIAS). Theor Appl Genet 72: 27–32

Fukui K (1996) Plant chromosomes at mitosis. In: Fukui K, Nakayama S (eds) Plant chromosomes: laboratory methods. CRC Press, Boca Raton, Florida, pp 1–17

Fukui K, Iijima K (1991) Somatic chromosome map of rice by imaging methods. Theor Appl Genet 81: 589–596

Fukui K, Iijima K (1992) Manual on rice chromosomes (2nd edn.). Misc Publ Natl Inst Agrobiol Resour 4: 1–25

Fukui K, Mukai Y (1988) Condensation pattern as a new image parameter for identification of small chromosomes in plants. Jpn J Genet 63: 359–366

Fukui K, Kamisugi Y, Sakai F (1994) Physical mapping of 5S rDNA loci by direct-cloned biotinylated probes in barley chromosomes. Genome 37: 105–111

Fukui K, Nakayama S, Ohmido N, Yoshiaki H, Yamabe M (1998) Quantitative karyotyping of three diploid *Brassica* species by imaging methods and localization of 45S rDNA loci on the identified chromosomes. Theor Appl Genet 96: 325–330

Fulneček J, Matyášek R, Kovařik A, Bezděk M (1998) Mapping of 5-methylcytosine residues in *Nicotiana tabacum* 5S rRNA genes by genomic sequencing. Mol Gen Genet 259: 133–141

Gerstel DU (1960) Segregation in new allopolyploids of *Nicotiana*. I. Comparison of 6× (*N. tabacum* × *tomentosiformis*) and 6× (*N. tabacum* × *otophora*). Genetics 45: 1723–1734

Gerstel DU (1963) Segregation in new allopolyploids of *Nicotiana*. II. Discordant ratios from individual loci in 6× (*N. tabacum* × *N. sylvestris*). Genetics 48: 677–689

Goodspeed TH (1954) The genus *Nicotiana*. Chronica Botanica Company, Waltham, Massachusetts

Gray JC, Kung SD, Wildman SG, Sheen SJ (1974) Origin of *Nicotiana tabacum* L. detected by polypeptide composition of Fraction I protein. Nature 252: 226–227

Ha S, Moore PH, Heinz D, Kato S, Ohmido N, Fukui K (1999) Quantitative chromosome map of the polyploid *Saccharum spontaneum* by multicolor fluorescence in situ hybridization and imaging methods. Plant Mol Biol 39: 1165–1173

Hanson RE, Islam-Faridi MN, Percival EA, Crane CF, Ji Y, McKnight TD, Stelly DM, Price HJ (1996) Distribution of 5S and 18S-28S rDNA loci in a tetraploid cotton (*Gossypium hirsutum* L.) and its diploid ancestors. Chromosoma 105: 55–61

Hizume M (1994) Allodiploid nature of *Allium wakegi* Araki revealed by genomic in situ hybridization and localization of 5S and 18S rDNAs. Jpn J Genet 69: 407–415

Ito M, Ohmido N, Akiyama Y, Fukui K, Koba T (2000) Characterization of spinach chromosomes by condensation patterns and physical mapping of 5S and 45S rDNAs by FISH. J Am Soc Hort Sci 125: 59–62

Kamisugi Y, Furuya N, Iijima K, Fukui K (1993) Computer-aided automatic identification of rice chromosomes by image parameters. Chrom Res 1: 189–196

Kato S, Fukui K (1998) Condensation pattern (CP) analysis of plant chromosomes by an improved chromosome image analysing system, CHIAS III. Chrom Res 6: 473–479

Kato S, Hirose T, Akiyama Y, O'Neill CM, Fukui K (1997) Manual on the chromosome image analyzing system III, CHIAS III. Res Rep Agr Develop Hokuriku Area 36: 1–76

Kenton A, Parokonny AS, Gleba YY, Bennett MD (1993) Characterization of the *Nicotiana tabacum* L. genome by molecular cytogenetics. Mol Gen Genet 240: 159–169

Kitamura S, Inoue M, Ohmido N, Fukui K (1997) Identification of parental chromosomes in the interspecific hybrids of *Nicotiana rustica* L. × *N. tabacum* L. and *N. gossei* Domin × *N. tabacum* L., using genomic in situ hybridization. Breed Sci 47: 67–70

Merritt JF (1974) The distribution of heterochromatin in the genus *Nicotiana* (Solanaceae). Am J Bot 61: 982–994

Moscone EA, Matzke MA, Matzke AJM (1996) The use of combined FISH/GISH in conjunction with DAPI counterstaining to identify chromosomes containing transgene inserts in amphidiploid tobacco. Chromosoma 105: 231–236

Murray MG, Thompson WF (1980) Rapid isolation of high-molecular-weight plant DNA. Nucleic Acids Res 8: 4321–4325

Nakayama S, Fukui K (1997) Quantitative chromosome mapping of small plant chromosomes by improved imaging on CHIAS II. Genes Genet Syst 72: 35–40

Ogura H (1980) Cytogenetic studies on a recently identified *Nicotiana* species, *N. kawakamii* Ohashi. Cytologia 45: 33–42

Okamuro JK, Goldberg RB (1985) Tobacco single-copy DNA is highly homologous to sequences present in the genomes of its diploid progenitors. Mol Gen Genet 198: 290–298

Parokonny AS, Kenton AY (1995) Comparative physical mapping and evolution of the *Nicotiana tabacum* L. karyotype. In: Brandham PE, Bennett MD (eds) Kew Chromosome Conference IV. Royal Botanic Gardens, Kew, pp 301–320

Reed SM (1991) Cytogenetic evolution and aneuploidy in *Nicotiana*. In: Tsuchiya T, Gupta PK (eds) Chromosome engineering in plants: genetics, breeding, evolution, part B. Elsevier, The Netherlands, pp 483–505

Sheen SJ (1972) Isozymic evidence bearing on the origin of *Nicotiana tabacum* L. Evolution 26: 143–154

Shishido R, Apisitwanich S, Ohmido N, Okinaka Y, Mori K, Fukui K (1998) Detection of specific chromosome reduction in rice somatic hybrids with the A, B, and C genomes by multi-color genomic in situ hybridization. Theor Appl Genet 97: 1013–1018

Takaiwa F, Oono K, Sugiura M (1984) The complete nucleotide sequence of a rice 17S rRNA gene. Nucleic Acids Res 12: 5441–5448